Centralized model predictive control of the wastewater treatment plant of Seine-Aval

A. Ben Ayed
ICTEAM, UCLouvain
Louvain-la-Neuve, Belgium
ayoub.benayed@uclouvain.be

D. Dochain
ICTEAM, UCLouvain
Louvain-la-Neuve, Belgium
denis.dochain@uclouvain.be

I. Prodan
Univ. Grenoble Alpes, Grenoble INP, LCIS
F-26000, Valence, France
ionela.prodan@lcis.grenoble-inp.fr

C.E. Robles-Rodriguez
TBI, Université de Toulouse
CNRS, INRAE, INSA, Toulouse, France
roblesro@insa-toulouse.fr

***Abstract*—This study concentrates on the control of the largest European wastewater treatment plant (WWTP), Seine-Aval (SAV). This WWTP can be viewed as the interconnection of multiple unit operations. We start by deriving the dynamical models of the wastewater treatment units on the basis of mass balances and inspired from the activated sludge model (ASM) of the IWA. The model is then used to design a centralized controller with the objective to meet the wastewater European directives constraints. The identification of the model parameters and the controller design are based on two years of data collected at SAV. The centralized controller has been tuned and evaluated with three scenarios that consider dry, rainy and stormy weathers. The results show that WWTP performance are improved by 50 percent in dry weather (10 percent in the rain) while observing new European water policies and reducing the need and costs in reactants. The model definition and problem formulation allow to account for more complex phenomena in the future.**

***Index Terms*—Wastewater treatment, dynamical modelling, centralized control**

I. Introduction

After the two European Directives 91/271 and 98/15 for wastewater treatment, the Water Framework Directive (WFD) 2000/60 comes with a larger notion of river basins. In particular it imposes the good chemical and ecological states of both the surface and ground waters.

The SIAAP (Syndicat Interdépartemental pour l'Assainissement de l'Agglomération Parisienne) is in charge of collecting and treating the wastewater of the city of Paris and its suburbs via a network of 6 wastewater treatment plants and 440km of sewers. This area covers 79000 km^2, which corresponds to 13% of the French territory and about 30% of the French population. The largest plant is Seine-Aval (SAV) which treats around 17 Mm^3 of wastewater per day (80% of the wastewaters of Paris and of its suburbs), which is the object of this paper. In case of extreme events (heavy rains, storms), it may happen that the level of some components to be treated, typically nitrogen, goes over the required threshold.

Over the years, some effort has been made to use model predictive control (MPC) in the control of WWTPs. Simultaneous design and control strategies with MPC has been proposed in [1] and [2]. In [3], 8 different control strategies were designed to improve nutrient removal of the Benchmark Simulation Model No.1 (BSM1). Hierarchical [4] and supervised [5] MPC control strategies have been proposed to accommodate a wide range of operating conditions as storm weather and heavy pollutant load for instance. All papers highlight the MPC difficulties to manage such complex processes with strong nonlinearities, large variable time constant and continuous perturbation of the input influent [6]. This leads to high evaluation time and makes the online implementation of the MPC to be intractable, or to limit the management of the plant to only few control variables [7].

The objective of this work is to illustrate that centralized model predictive control may improve the performance of the whole plant while meeting the WFD requirements regardless of the weather conditions. This control strategy is aimed at serving as a benchmark framework to build more complex control strategies. In this context, a model that represents the main variables and captures the dynamics of the main variables is needed for control design. Moreover, the methodology and structural definition of the system is made so it can be easily extended in further work, for example by taking into account more complex phenomena or add new treatment units.

The paper presents the derivation and the model parameter identification of the dynamical model for the unit operations of the Seine-Aval WWTP on the basis of mass balances and inspired from the activated sludge model (ASM) of the IWA [8].

The paper is organized as follows. First the general structure and operation of the SAV WWTP is presented. Section 2 details the model parameter identification. Section 3 and 4 present the design of the centralized control and illustrate its performance in numerical simulation.

II. Modeling of the WWTP

A. Description of Seine Aval

The wastewater entering SAV undergoes a pretreatment that consists of removing large solid particles, sand and oil by pre-screening, grid removal and de-oiling. After pretreatment, the wastewater treatment is performed in two steps: carbon and phosphorus removal (via physico-chemical lamella settling) and nitrogen removal (via a biofiltration unit). Additionally to the two steps, SAV has a parallel membrane bioreactor unit which can treat up to 3.5 $\mathrm{Mm^3 d^{-1}}$ of wastewater representing 15% of the total nominal flow rate. The general structure of the treatment process is schematized in Fig. 1.

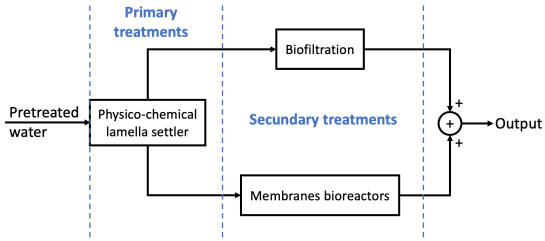

Fig. 1. General structure of the Seine-Aval WWTP

In this paper, we focus on the biofiltration pathway because the flow rate in the membrane bioreactor unit is kept constant and is small as compared to the entire WWTP flow rate. The biofiltration consists of successive units of pre-denitrification, nitrification and post-denitrification. Each of these steps is divided in a large number of units in parallel and/or in series that can be disabled (e.g. for maintenance), possibly with different flow rates. However in practice, the unit operations treat equally distributed flow rates. For this reason, we consider only one equivalent tank for each treatment step. The volume of these equivalent reactors is considered constant since no retention mechanisms are observed. Due to its low fluctuations as compared to the other components, microbial population can also be assumed constant.

Fig. 2 shows the considered part of Seine-Aval and the interconnections between the units. Black, red and blue arrows indicates normal, bypassed and recirculated flow path for wastewater, respectively. u_i^f are the flow rates that can possibly be used as control variables, and R_i are the discharge flow rates, both in $\mathrm{m^3\ d^{-1}}$. u_i^r are the inlet reactant control variables ($\mathrm{m^3\ d^{-1}}$, except for the settling unit which is a concentration and is measured in $\mathrm{g\ m^{-3}}$), and $u^T = [u^f\ u^r]$. $\xi_{i\bullet}$ is the state vector for reactor i. It is composed successively of the concentration of the total suspended solid (TSS), phosphate (PO_4), chemical oxygen demand (COD), ammonium (NH_4), nitrite (NO_2), nitrate (NO_3) and dissolved oxygen (O_2), all expressed in $\mathrm{g\ m^{-3}}$. For instance, ξ_{24} denotes the concentration of ammonium in the pre-denitrification unit. The considered states are the ones that are measured in the units and correspond to most important variables to respect to the WFD. Q_{in} and Q_{out} ($\mathrm{m^3\ d^{-1}}$) are the inlet and outlet flow rates of the WWTP, respectively. C_{in} and y ($\mathrm{g\ m^{-3}}$) are the inlet and outlet concentrations of the WWTP, respectively.

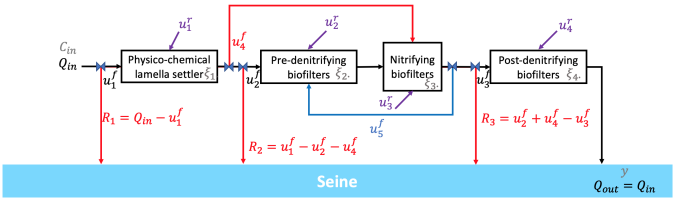

Fig. 2. Representation of the considered part of the WWTP of Seine-Aval

B. Model description

The dynamics of the concentrations are in the form of the *General Dynamical Model* for continuous stirred tank reactors [9]:

$$\frac{d\xi}{dt} = -D\xi + Kr(\xi) + F - Q = f(\xi, u, C_{in}) \qquad (1)$$

where $-D\xi + F - Q$ correspond to transport dynamics and Kr denotes the conversion term. More specifically, K is the yield coefficient matrix (see Table I) while $r(\xi)$ is the reaction rate vector (see Table II). D, F and Q are the dilution rate matrix, the feed rate vector and the gaseous outflow rate vector, respectively.

TABLE I
YIELD COEFFICIENT MATRIX K

process → / ↓ nutrients	1	2	3	4	5	6	7	8	9
ξ_{11}	-1								
ξ_{12}		-1							
ξ_{13}			-1						
ξ_{23}				$\frac{-1}{Y_1}$	$\frac{-1}{Y_2}$				
ξ_{25}				$\frac{1}{Y_3}$	1				
ξ_{26}				-1					
ξ_{34}						-1			
ξ_{35}						$\frac{1}{Y_4}$	-1		
ξ_{36}							$\frac{1}{Y_5}$		
ξ_{37}						$\frac{-1}{Y_6}$	$\frac{-1}{Y_7}$		
ξ_{43}								$\frac{-1}{Y_8}$	$\frac{-1}{Y_9}$
ξ_{45}								$\frac{1}{Y_{10}}$	-1
ξ_{46}								-1	

Denitrification units are fed with phosphoric acid H_3PO_4 and methanol CH_3OH (with volumic mass ρ_1) in order to cover the needs in phosphate for the biomass and in carbon for the denitrification. Aeration is modelled by the oxygen transfer rate relation where O_2^* is the oxygen saturation constant (mgO_2/L), k_La the oxygen liquid-gas transfer coefficient ($\mathrm{d^{-1}}$), and Q_{ref} the reference flow ($\mathrm{m^3\ d^{-1}}$).

The principle of physico-chemical lamella settler is based on the sedimentation and separation of insoluble solid particles from the wastewater due to gravity. Ferric chloride $FeCl_3$ and

TABLE II
REACTION RATE EQUATIONS

	Reaction	Kinetics equation
1	Settling of TSS	$k_0 \frac{\xi_{11} u_1^r}{K_{FeCl_3} + u_1^r}$
2	Phosphate precipitation	$k_1 \frac{\xi_{12} u_1^r}{K_{PO_4} + \xi_{12}}$
3	COD removal	$k_2\ \xi_{13}\ FeCl_3$
4	Pre-denit. of NO_3 by heterotrophic bacteria X_1	$\mu_{1,max}\ \frac{\xi_{26}}{K_{NO_3,1}+\xi_{26}}\ \frac{\xi_{23}}{K_{COD,1}+\xi_{23}} X_1$
5	Pre-denit. of NO_2 by heterotrophic bacteria X_1	$\mu_{2,max} \frac{\xi_{25}}{K_{NO_2,1}+\xi_{25}}\ \frac{\xi_{23}}{K_{COD,2}+\xi_{23}} X_1$
6	Aerobic nitrification by *Nitrosomonas* bacteria X_2	$\mu_{3,max} \frac{\xi_{34}}{K_{NH_4}+\xi_{34}}\ \frac{\xi_{37}}{K_{O_2,1}+\xi_{37}} X_2$
7	Aerobic nitrification by *Nitrobacter* bacteria X_3	$\mu_{4,max} \frac{\xi_{36}}{K_{NO_2,2}+\xi_{36}}\ \frac{\xi_{37}}{K_{O_2,2}+\xi_{37}} X_3$
8	Post-denit. of NO_3 by heterotrophic bacteria X_4	$\mu_{5,max}\ \frac{\xi_{46}}{K_{NO_3,2}+\xi_{46}}\ \frac{\xi_{43}}{K_{COD,3}+\xi_{43}} X_4$
9	Post-denit. of NO_2 by heterotrophic bacteria X_4	$\mu_{6,max} \frac{\xi_{45}}{K_{NO_2,3}+\xi_{45}}\ \frac{\xi_{43}}{K_{COD,4}+\xi_{43}} X_4$

an anionic polymer are also added to allow the settling of colloidal particle via coagulation and flocculation mechanism. This also results in the precipitation of phosphate.

The settling rate of the total suspended solids is assumed to be first order with respect to TSS with Monod saturation in $FeCl_3$ (with a half-saturation constant K_{FeCl_3}) (Table II - reaction 1). The phosphate consumption rate is also considered to be first order with respect to ferric chloride (with a kinetic constant k_1), and Monod for PO_4 (with a half-saturation coefficient K_{PO_4}) (Table II - reaction 2). The consumption rate for chemical oxygen demand is considered to be first order with respect to COD and $FeCl_3$ (with a kinetic constant k_2) (Table II - reaction 3). The denitrification is concerned with both the pre- and post-denitrification and consists in the reduction of the nitrates NO_3^- in the wastewater into nitrogen gas N_2 by heterotrophic bacteria X_1 and X_4. These bacteria in anoxic conditions will take from the nitrates the oxygen necessary for their growth in presence of assimilable carbon CH_2O. The denitrification process proceeds in two steps:

$$NO_3^- \rightarrow NO_2^- \rightarrow N_2$$

Denitrification kinetics are characterized by double Monod equations with respect to nitrate and COD (Table II - reactions 4 and 8), and with respect to nitrite and COD (Table II - reactions 5 and 9), respectively. Finally the nitrification consists in the transformation of the dissolved ammonia (ammoniacal hydrogen NH_4^+ and organic N_{orga}) into nitrite (Table II - reaction 6) and nitrate (Table II - reaction 7). For the last reaction rate equations (Table II - reactions 4 to 9), μ_{max} and K are the maximum specific growth rate and the half-saturation constant, respectively.

C. Parameter identification

The parameters of the model for physico-chemical lamella settling have been calibrated and validated based on 2 years of daily data from Seine-Centre (SEC) units. Indeed the settling units of SAV are still under construction while there is no available sensor at the present time in the existing units. The data cover a period from March 2010 to 2011 and March 2013 to 2014. Output measurements had been linearly interpolated whenever data were missing. For the biofiltration units, 9 months of daily and 15 minutes period data were available to calibrate and validate the models. The data cover a period from August 2018 to May 2019. The 15 minutes data were averaged on daily period in order to accommodate for the large noise of the sensors and unify the time scale. Two third of each data sets have been carefully selected for the calibration; one third at the beginning and another third at the end of the set. The last third data set had been used for validation. Every unit has been calibrated individually.

Parameter calibration has been performed using the following procedure:

1) Yield coefficients are first identified on the basis of the General Dynamical Model structure and the notion of reaction invariants [9] that allows the identification of the yield coefficients independently of the kinetic parameters.

2) Similarly oxygen parameters are also identified with linear regressions independently of the kinetic parameters.

3) kinetic parameters lead to models that are nonlinear in the parameters. Those parameters have been identified based on Levenberg-Marquardt algorithm. The calibrated values for the different models are reported on the Table III.

TABLE III
CALIBRATED PARAMETERS

Parameter	Value	CI	Typ.val.	Unit
Y_1	0.077	[0.04; 0.69]	0.2	$gNO_2/gCOD$
Y_2	0.14	[0.11; 0.18]	0.3	$gNO_3/gCOD$
Y_3	40.57	[22.2; 235]	1	gNO_3/gNO_2
Y_4	6.87	[4.55; 9.2]	1	gNH_4/gNO_2
Y_5	0.14	[0.09; 0.20]	0.33	gNO_2/gNO_3
Y_6	$3.19\ 10^5$	$[-\infty; -\infty]$	0.3	gNH_4/gO_2
Y_7	$1.67\ 10^5$	$[-\infty; -\infty]$	0.3	gNO_2/gO_2
Y_8	0.25	[0.17; 0.45]	0.2	$gNO_2/gCOD$
Y_9	0.96	[0.64; 1.92]	0.3	$gNO_3/gCOD$
Y_{10}	27.57	[20.2; 43.6]	1	gNO_3/gNO_2
$\mu_{1,max}$	0.072	[0.044; 0.099]	3	$gNO_3/gX_1\ d^{-1}$
$\mu_{2,max}$	50.8	$[-4.39; 4.39]\ 10^5$	3	$gNO_2/gX_1\ d^{-1}$
$\mu_{3,max}$	1.67	[1.5; 1.84]	0.9	$gNH_4/gX_3\ d^{-1}$
$\mu_{4,max}$	0.88	[0.78; 0.96]	0.65	$gNO_2/gX_3\ d^{-1}$
$\mu_{5,max}$	576.97	[184; 970]	3	$gNO_3/gX_4\ d^{-1}$
$\mu_{6,max}$	0.31	[−7.27; 7.89]	3	$gNO_2/gX_4\ d^{-1}$
k_0	82.85	[68.1; 97.6]	-	d^{-1}
k_1	2.04	[1.88; 2.19]	1	$gPO_4/gFeCl_3\ d^{-1}$
k_2	1.4	[1.32; 1.47]	-	$m^3/gFeCl_3\ d^{-1}$
K_{PO_4}	0.0346	[−4.89; 4.89]	-	$gPO_4\ m^{-3}$
K_{FeCl_3}	$6.65\ 10^{-7}$	[0.021; 0.048]	-	$gFeCl_3\ m^{-3}$
$K_{COD,1}$	$2.75\ 10^{-5}$	[−21; 21]	0.1	$gCOD\ m^{-3}$
$K_{COD,2}$	$8.24\ 10^5$	$[-7.12; 7.12]\ 10^9$	0.1	$gCOD\ m^{-3}$
$K_{COD,3}$	70.29	[−7.88; 148]	0.1	$gCOD\ m^{-3}$
$K_{COD,4}$	0.001	[−806; 806]	0.1	$gCOD\ m^{-3}$
K_{NH_4}	0.01	[−0.33; 0.53]	0.14	$gNH_4\ m^{-3}$
$K_{NO_2,1}$	$2.68\ 10^{-11}$	[−0.063; 0.063]	0.5	gNO_2/m^{-3}
$K_{NO_2,2}$	0.01	$[-1.42; 3.59]\ 10^{-2}$	0.28	$gNO_2\ m^{-3}$
$K_{NO_2,3}$	$4.42\ 10^{-8}$	[−5.30; 5.30]	0.5	$gNO_2\ m^{-3}$
$K_{NO_3,1}$	0.1	[−0.14; 0.34]	0.5	$gNO_3\ m^{-3}$
$K_{NO_3,2}$	0.1	[−0.0077; 0.21]	0.5	$gNO_3\ m^{-3}$
$K_{O_2,1}$	$1.501\ 10^{-4}$	$[-2.25; 2.25]\ 10^3$	0.8	$gO_2\ m^{-3}$
$K_{O_2,2}$	$4.42\ 10^{-13}$	[−0.7; 0.7]	0.8	$gO_2 m^{-3}$
k_La	0.55	[0.41; 0.70]	-	d^{-1}

The average retention time for the wastewater in the settler is around 3.6 hour ($1/k_0$). This is reasonable considering the actual sludge retention time in the settler. Furthermore the saturation constant for TSS removal is low, meaning the saturation does not depend on $FeCl_3$. This was expected since $FeCl_3$ is overdosed most of the time.

The reactions taking place in pre and post-denitrification units are the same, however the kinetic parameters and yield coefficients are noticeably different. Globally post-denitrification is more effective in the nitrate removal. Moreover the two units differs by the fixed media where the bacteria are growing; Biostyr filters for pre-denitrification and Biofor filters for post-denitrification. For both units, the high value for Y_3 and Y_{10} shows that only a fraction ($<5\%$) of nitrate is converted into nitrite. This suggests problems in the nitrite measurements, the existence of other intermediates or a direct transformation of nitrate into N_2. Moreover nitrite removal does not saturate with COD and does not depend on NO_2 leading to first order kinetics with respect to COD.

For the nitrification unit, the saturation constants for oxygen are negligible, meaning the oxygen is always saturated. This is expected since oxygen is supplied in excess by the aeration. Moreover the high yield coefficients in oxygen leads to a very small consumption of oxygen. This suggests that daily data are not able to describe the evolution of dissolved oxygen accurately; which results in an underestimation of the k_La parameter. The validation results in dry weather (see section IV.A) are shown in Fig. IV where there is a good agreement between experimental data and the model.

III. Control design

Currently control is implemented so as to treat a maximum of wastewater, the units are managed independently, and the reactants are overdosed most of the time. For instance in the settling unit ferric chloride is added with excess, leading to an overtreatment of phosphate. As a result H_3PO_4 must generally be added in pre-denitrification to handle the need in phosphate of the biomass. Furthermore SAV is not yet subjected to the WFD; so no concrete strategy has been put in place for it.

The objective is to find the optimal distribution of the wastewater flow rate within the plant, especially in presence of extreme events. Moreover the control of added reactants (i.e. ferric chloride, methanol and oxygen) should lead to a reduction of the operating costs while fulfilling the constraints. These latter include physical and technical constraints on inputs and outputs (imposed by the UWWD (EU directive 98/15) and WFD). WFD constraints expressed in terms of the concentrations in the river basin have been transposed at the output of the WWTP considering nominal flow rate and concentration in the Seine. All the constraints are summarized in Table IV.

TABLE IV
Input and output constraints

	Description	Constraints
1	Positive system	$u \geq 0$
2	Max dec. input flow	$u_1^f \leq 2.25$ [Mm^3 d^{-1}]
3	Max pre-dnit. input flow	$u_2^f + u_5^f \leq 2.7$ [Mm^3 d^{-1}]
4	Max nit. input flow	$u_2^f + u_4^f + u_5^f \leq 4.6$ [Mm^3 d^{-1}]
5	Max post-dnit. input flow	$u_3^f \leq 1$ [Mm^3 d^{-1}]
6	Positive rej. flow R_1	$Q_{in} - u_1^f \geq 0$
7	Positive rej. flow R_2	$u_1^f - u_2^f - u_4^f \geq 0$
8	Positive rej. flow R_3	$u_2^f + u_4^f - u_3^f \geq 0$
9	$FeCl_3$ conc. limits	$23 \leq u_1^r \leq 39$ [g$FeCl_3$ m^{-3}]
10	Pre-dnit max meth. flow	$u_2^r \leq 1$ [km^3 d^{-1}]
11	Aeration flow limits	$2.8 \leq u_3^r \leq 8$ [Mm^3 d^{-1}]
12	Post-dnit max meth. flow	$u_4^r \leq 0.1$[km^3 d^{-1}]
13	UWWD on TSS	$y_1 \leq 30$ [gTSS m^{-3}]
14	UWWD on PO_4	$y_2 \leq 1$ [gPO_4 m^{-3}]
15	UWWD on COD	$y_3 \leq 90$ [gCOD m^{-3}]
16	UWWD on NH_4	$y_4 \leq 5$ [gNH_4 m^{-3}]
17	UWWD on Global Nitrogen	$y_4 + y_5 + y_6 \leq 10$ [gN m^{-3}]
18	WFD on TSS	$y_1 \leq 460$ [gTSS m^{-3}]
19	WFD on PO_4	$y_2 \leq 0.5$ [gPO_4 m^{-3}]
20	WFD on COD	$y_3 \leq 130$ [gCOD m^{-3}]
21	WFD on NH_4	$y_4 \leq 3$ [gNH_4 m^{-3}]
22	WFD on NO_2	$y_5 \leq 1.6$ [gNO_2 m^{-3}]
23	WFD on NO_3	$y_6 \leq 320$ [gNO_3 m^{-3}]
24	WFD on O_2	$y_7 \geq 6$ [gO_2 m^{-3}]

A. Problem formulation

We linearise the system around a nominal working point (ξ_N, u_N, $C_{in,N}$, y_N) for each scenario and discretize it using the first-order hold method:

$$\xi[k+1] \quad = \quad \xi[k] + \frac{d\xi}{dt}\Delta t \tag{2}$$

where Δt is the sampling period. This lead us to the following linear discrete model:

$$\begin{aligned} \xi[k+1] &= A_d\,\xi[k] + B_{ud}\,u[k] + B_{vd}\,C_{in}[k] + \xi_{diff} && (3)\\ y[k] &= C_d\,\xi[k] + D_{ud}u[k] + D_{vd}\,C_{in}[k] + y_{diff} && (4) \end{aligned}$$

with

$$\begin{aligned} A_d &= \Delta t\,\frac{\partial f}{\partial \xi}\bigg|_{\xi_N,u_N,C_{in,N}} + \begin{pmatrix} 1 & & \\ & \ddots & \\ & & 1 \end{pmatrix} && (5)\\ B_{ud} &= \Delta t\,\frac{\partial f}{\partial u}\bigg|_{\xi_N,u_N,C_{in,N}},\ B_{vd} = \Delta t\,\frac{\partial f}{\partial C_{in}}\bigg|_{\xi_N,u_N,C_{in,N}} && (6)\\ C_d &= \frac{\partial g}{\partial \xi}\bigg|_{\xi_N,u_N,C_{in,N}} && (7)\\ D_{ud} &= \frac{\partial g}{\partial u}\bigg|_{\xi_N,u_N,C_{in,N}},\ D_{vd} = \frac{\partial g}{\partial C_{in}}\bigg|_{\xi_N,u_N,C_{in,N}} && (8)\\ \xi_{diff} &= -A_d\xi_N - B_{ud}u_N - B_{vd}C_{in,N} && (9)\\ y_{diff} &= y_N - C_d\xi_N - D_{ud}u_N - D_{vd}C_{in,N} && (10) \end{aligned}$$

Beside reactant and environmental costs, a quadratic penalty on input variation $\Delta u[k]$, to avoid unstable behaviour of the controller, and a slack variable ϵ to soften output constraints, have been added. This latter is necessary to ensure the existence of a solution. In fact, output constraints cannot be met in each circumstance, e.g. in extreme weather conditions. The final expression of the problem is formulated in the form of model predictive control:

$$\min_u J = \sum_{i=1}^{N_{pred}} c\,u[k] + w_y\,y[k] + \Delta w_{du}\,(\Delta u[k])^2 + \epsilon \tag{11}$$

$$w.r. \begin{cases} \xi[k+1] = A_d\,\xi[k] + B_{ud}\,u[k] + B_{vd}\,C_{in}[k] + \xi_{diff} \\ y[k] = C_d\,\xi[k] + D_{ud}u[k] + D_{vd}\,C_{in}[k] + y_{diff} \\ F_u\,u + H_uQ_{in} \leq G_u \\ F_y\,y \leq G_y + \epsilon\,V_y \\ \epsilon \geq 0 \end{cases} \tag{12}$$

where N_{pred}, c, w_y, w_{du} are the prediction horizon, the reactant cost, the weight for nutrients rejection in the Seine

and the input variation weight, respectively. The weighting terms are normalising factors so that the objective function is dimensionless. Input constraints are synthetically described through matrix F_u, G_u and H_u. Output constraints are described through matrix F_y, G_y and V_y, this latter being the soft constraint weight vector. At each time step the controller computes the 9 optimal control inputs u from the measured 28 state concentrations, the 7 output concentrations, the constraints and the model prediction over the finite-time horizon.

IV. Simulation results

3 periods of 21 days each one have been considered: one in dry weather (from August 13 to 24, 2018 - scenario 1), one in rainy conditions (from December 8 to 29, 2018 - scenario 2) and one during a storm period (from January 12 to February 2, 2019 - scenario 3). The data have been selected from one year of daily measurements of the nutrient concentrations in each unit along with 15 minutes data of daily averaged flow rates. For the given data set, ferric chloride data are not available, a constant concentration of 32[g m^{-3}] has been extrapolated from SEC data. The controller performance has been assessed based on the first two terms of the objective function, i.e. the economical and environmental cost. The weights of these two terms, c and w_y, are operational parameters. They are chosen based on the SIAAP desired control strategies. The other controller parameters have been tuned to maximise the controller performance in dry weather. We first fix the sampling time Δt at 15 min as a compromise between discretisation error and time complexity. We then solve a reduced version of the problem without environmental cost, quadratic penalty on input variation and output constraint. The prediction horizon is then increased until no further improvement is found. Its threshold is close to the process time response, i.e. around 6 hours. We then add output constraints and the corresponding penalty terms. This leads to the expected improvements in the control behaviour. The weights V_y are set as a normalisation factor between the concentrations. The weights w_{du} are also first normalised and then tuned to smooth input variations. Starting from zero their weights are increased until the unstable behaviour is reduced.

$$
\begin{aligned}
c &= [0\,0\,0\,0\,0\,0.003125\,14.700\,125.31]^T \\
w_y &= [0.0028\,0.22\,0.0016\,0.025\,0.28\,0.023\,-0.06]^T \\
V_y &= [0.354\,0.0225\,0.94\,0.06\,0.021\,0.55\,0.066\,0.002] \\
w_{du} &= [0\,0\,0.001\,6\;10^{-4}\,6\;10^{-4}\,1.75\,0\,15]^T
\end{aligned}
$$

The different tests are summarized in Table V where $\bar{F_{obj}}$ denotes the mean value of the objective function. In general, centralized control allows to achieve better treatment performance; the gain is really noticeable in dry weather with 50 percent of improvement versus 10 percent in the rainy period. In rainy periods, nutrients are more diluted, leading to lower degree of freedom for the controller. Between day 15 and 17, an extreme event occurs, and the inlet flow rate increases by a factor of 2 (Fig. IV).

TABLE V
Scenario results

Scenario	Δt	N_{pred}	Input const.	Output const.	c	w_{du}	$\bar{F_{obj}}$	Sim. time [s]
1			experimental data				1.16	-
1	15 min.	12 Δt	yes	no	no	no	1.0317	72.75
1	15 min.	24 Δt	yes	no	no	no	0.8632	90
1	15 min.	48 Δt	yes	no	no	no	0.8632	197
1	15 min.	96 Δt	yes	no	no	no	0.8632	495
1	15 min.	2 Δt	yes	no	no	no	0.7349	58.6
1*	15 min.	24 Δt	yes	yes	yes	yes	0.5480	662
1	15 min.	24 Δt	yes	yes	no	yes	0.50	160
2			experimental data				1.24	-
2	15 min	24 Δt	yes	yes	yes	yes	1.1	666
3			experimental data				1.41	-
3	15 min	24 Δt	yes	yes	yes	yes	1.41	1050

In dry weather, we note that adding methanol (u_2^r and u_4^r) is not necessary to achieve the desired objectives. Instead one can act on the pre-denitrification inlet (u_2^f), recirculation (u_5^f) and bypass (u_4^f) flow rates to increase the performance of the pre-denitrification. This unit is only efficient in the treatment of nitrite and nitrate after the nitrification through the recirculation. In fact, the inlet concentrations at the input of the station and after the settling is close to zero. In rainy and storm period, the inlet flow rate is higher, recirculation is limited so that adding methanol is unavoidable. In the nitrification unit, the air flow rate (u_3^r) has to be increased to its maximum allowable value to accommodate the stronger constraints on ammonia and dissolved oxygen defined in the WFD. The time evolution of the concentrations is represented on Fig. IV. It shows in particular that ammonia and nitrite can be efficiently reduced while keeping nitrate around the same level and increasing dissolved oxygen.

Acknowledgment

This research is supported by a FRIA scholarship (F.R.S.-FNRS).

References

[1] M. Rafiei-Shishavan, S. Mehta, and L.A. Ricardez-Sandoval, "Simultaneous design and control under uncertainty: A back-off approach using power series expansions," Comput. Chem. Eng., 2017, 99, pp. 66–81.

[2] B.E. Rodríguez-Pérez, A. Flores-Tlacuahuac, L. Ricardez-Sandoval, and F.J. Lozano, "Optimal water quality control of sequencing batch reactors under uncertainty," Ind. Eng. Chem. Res., 2018, 57, pp. 9571–9590.

[3] A.G. Shiek, V.R.K. Machavolu, M.M. Seepana, and S.R. Ambati, "Design of control strategies for nutrient removal in a biological wastewater treatment process," Environ. Sci. Pollut. Res., 2021, 28, pp. 12092–12106.

[4] R. Piotrowski, H. Sawicki, and K. Zuk, "Novel hierarchical nonlinear control algorithm to improve dissolved oxygen control in biological WWTP," Journal of Process Control, 2021, 105, pp. 78–87.

[5] M. Grochowski, and T.A. Rutkowski, "Supervised model predictive control of wastewater treatment plant," 2016 21st International Conference on Methods and Models in Automation and Robotics.

[6] G. Harja, G. Vlad, and I. Nascu, "MPC advanced control of dissolved oxygen in an activated sludge wastewater treatment plant," 2016 IEEE International Conference on Automation, Quality and Testing, Robotics, pp. 1-6.

[7] A. Zhang, and J. Liu, "Economic MPC of Wastewater Treatment Plants Based on Model Reduction," Processes, 2019, 7, 10, 682.

[8] M. Henze, G. Maraisand and M. Vanloosdrecht, "Activated Sludge Model No.2d, ASM2d," Water Science and Technology, 1, 1989, pp. 165-182.

[9] G. Bastin and D. Dochain, "On-line Estimation and Adaptive Control of Bioreactors," Elsevier, 1990.

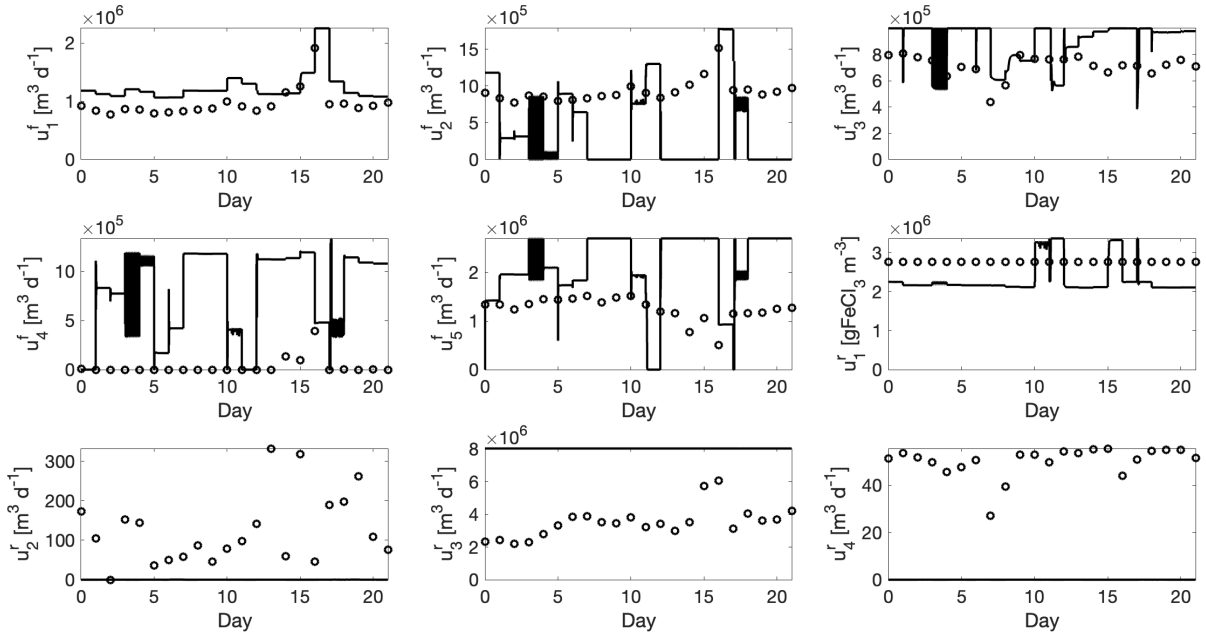

(—) centralized control (o) experimental data

Fig. 3. Inputs of the control for scenario 1*

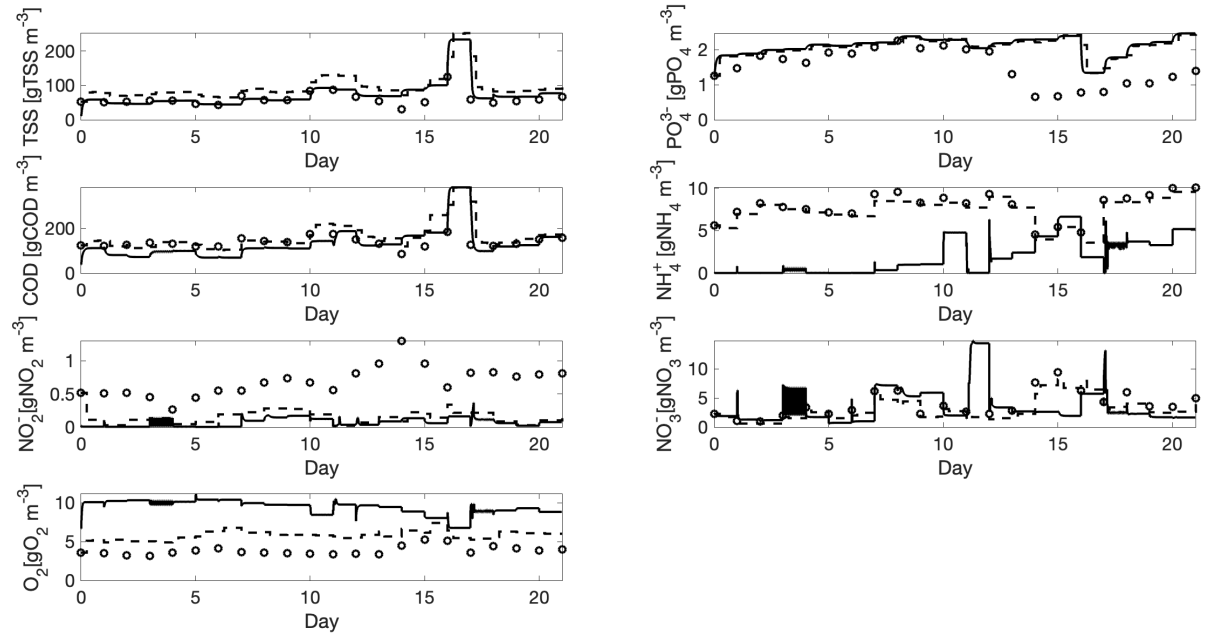

(—) centralized control (- -) non-linear model (o) experimental data

Fig. 4. Output concentrations for scenario 1*